

Zhen Cao
Levent Yobas

Department of Electronic and
Computer Engineering, Hong
Kong University of Science and
Technology, Clear Water Bay,
Kowloon, Hong Kong

Received January 24, 2013
Revised February 13, 2013
Accepted February 18, 2013

Research Article

Microchannel plate as a novel bipolar electrode for high-performance enrichment of anions

Microchannel plate (MCP), a high-porosity glass membrane used as an electron multiplier in analytical/scientific instruments for the detection of energetic photons and charged particles is demonstrated here as a highly effective bipolar electrode (BPE) for electrokinetic focusing of anions. Assembled between a pair of microfluidic channels filled with an electrolyte buffer and subjected to a sufficient bias potential, MCP supports faradaic reactions, owing to its semiconducting characteristics. Thousands of microcapillary tubes fused together define MCP and act in unison such that each microcapillary serves as a tiny BPE surrounding an infinitesimal element of bulk electrolyte with a large surface-area-to-volume ratio and hence performs highly effective as compared to a planar electrode inlaid into a microchannel. This performance has been validated here where concentration enrichment of a fluorescent tracer has been demonstrated at a remarkable rate of up to 175-fold/s exceeding those reported for planar BPEs. We attribute such high performance to the rapid onset of ion-depletion zone and subsequent steep field gradient, signifying the high-porosity structure of MCP as an effective BPE.

Keywords:

Bipolar electrode/ Concentration enrichment/ Lab on a chip/ Microchannel plate/
Microfluidics
DOI 10.1002/elps.201300040



Additional supporting information may be found in the online version of this article at the publisher's web-site

1 Introduction

1.1 General aspects

The ability to precisely handle minute amounts of liquids (pL–nL) in channels with a size of tens to hundreds of micrometers (microchannels) is a key aspect of microfluidics and presents applications with many opportunities including great economy of sample and reagents, less reaction waste, rapid analysis time, cost effectiveness, high resolving power of separation, compactness and portability, high throughput, and the ability to multiplex and automate [1]. Such scaling, however, brings along the challenge of detecting analytes in

ultra-small sample volumes often at fairly low concentrations. This is particularly the case in optical detection whereby the small channel dimensions limit the optical pathlength and confronts the concentration LOD with a drastically low number of target analytes in such a short distance [2]. Hence, it is of utmost importance to leverage techniques for in situ enrichment of analyte concentration within a detection volume to bring it to adequate levels.

For a given sample, analyte enrichment, or preconcentration, can take place through numerous means inclusive of, but not limited to, solvent or liquid-phase extraction via phase transfer or molecular diffusion [3], SPE via adsorption or surface affinity interactions [4], semipermeable membrane stacking via size-based exclusion or ion concentration polarization (ICP) [5, 6], and those based on the principle of electrokinetic or sometimes hydrodynamic equilibrium [7–17]. The latter class of techniques is largely inherited from CE, known to scale well with microfluidics, and offers field-addressable retention and release of analytes irrespective of their chemistry. Among those, the prominent ones are IEF [7], field-amplified

Correspondence: Dr. Levent Yobas, Department of Electronic and Computer Engineering, Hong Kong University of Science and Technology, Clear Water Bay, Kowloon, Hong Kong
E-mail: eelyobas@ust.hk
Fax: +852-2358-1485

Abbreviations: BPE, bipolar electrode; EF, enrichment factor; FGF, field gradient focusing; FI²⁻, fluorescein; ICP, ion concentration polarization; MCP, microchannel plate; TGF, temperature gradient focusing

Colour Online: See the article online to view Figs. 1–4 in colour.

sample stacking [8, 9], ITP [10], and field gradient focusing (FGF) [11–17].

IEF is applicable to analytes with a well-defined pI and over an accessible range (3–11). This limits the utility of the technique to peptides and proteins, albeit, poorly soluble in their net-neutral state and hence tend to aggregate. Field-amplified sample stacking requires analytes in an electrolyte at a lower ionic strength (conductivity) than the surrounding buffer whereas ITP keeps them between the leading and trailing electrolytes. Preparation and precise injection of multiple electrolytes can become a technical hurdle. Moreover, highly unstable electrokinetic flows triggered by sharp conductivity gradients disturb these very gradients required for the enrichment. Judicious choice of leading and trailing electrolyte chemistry demands a priori knowledge of electrophoretic mobilities of sample ions.

FGF is a family of techniques whereby charged analytes are simultaneously separated and enriched by balancing the electrophoretic force gradient against a fixed convective force. Each analyte can then be focused at a unique site based on its electrophoretic mobility. These techniques are, unlike IEF, applicable to fully ionized species, and differ in their methods of establishing a spatially nonuniform electric field. Such methods may involve a buffer with a temperature-dependent ionic strength subjected to a temperature gradient focusing [11, 12], or a buffer with a conductivity gradient [13]. They may also use a buffer with a constant conductivity under an electric-field gradient in a channel nonuniformly shaped [14–16] or embedded with an array of addressable electrodes [17]. The latter is referred to as the dynamic or digital FGF. Implementation of these techniques, yet, may not be that straightforward due to the requirement of special buffer arrangements, channels packed with chromatographic media to reduce dispersions, or ion-permeable dialysis membranes to decouple the constant convective flow from major disturbances.

Bipolar electrode (BPE) focusing is a recent addition to the FGF family and involves neither a semipermeable membrane nor nanochannels but a simple channel with an embedded conductor [18]. BPE refers to a floating conductor isolated from any external circuitry and in a channel filled with an ionic solution subjected to an electric potential of a sufficient magnitude. The field gets suppressed in the vicinity of BPE as it shunts the majority current through electronic conduction, which overtakes ionic conduction owing to anionic and cationic reactions simultaneously triggered at its opposing ends, the so-called faradaic depolarization [19]. This, however, is accompanied by the build-up of an ion-depleted low-conductivity region in a pH-sensitive buffer neutralized upon reacting with the products of water electrolysis. In return, a spatially extended steep field gradient is established in the adjoining anodic segment. BPE enrichment occurs in this particular segment at a unique position where anionic analytes tend to focus as the bulk EOF is offset by the increase in electrophoretic force.

Crooks and colleagues provided valuable insights into the role of faradaic reactions in the formation of electric field

gradients and the onset of concentration enrichment [18–23]. Laws et al. demonstrated BPE enrichment of a fluorescent anionic tracer by a factor of nearly 500 [20]. Subsequently, Anand et al. reported 500 000-fold enrichment of a tracer within 150 min (56-fold/s) upon enhancing the slope of the field gradient via higher field strength and higher concentration buffer, both sustainable owing to a 12.5-fold reduction in microchannel height [23]. The authors also introduced a dual-channel design, which decouples the voltage drop across BPE from the voltage applied, allowing for a higher driving potential and a more rapid enrichment, 142 000-fold in ~ 33 min (71-fold/s). While all these gains originate from a simple microstrip electrode with a planar quasi-2D profile, further gain in performance can then be expected from a high-aspect ratio 3D electrode, albeit with demand of relatively complex fabrication process.

Here, we introduce the microchannel plate (MCP) as a novel 3D BPE in a simple preconcentration device. A high porosity compact glass membrane, MCP features a densely populated array of high-aspect ratio precision microcapillaries [24]. Originally developed for image intensifiers as a high-resolution electron amplification element, MCP, owing to its high gain and superior temporal and spatial resolution, is also extensively used in a broad spectrum of applications from TOF MS and X-ray imaging to night vision goggles for the detection of charged particles and energetic photons. Manufactured in a unique process involving a series of fiber-draw procedures borrowed from the fiber-optic technology, MCP packs cylindrical glass microcapillaries with smooth and straight sidewalls, a profile formidable to replicate through lithography-based etching. MCP is made of a lead glass and then reduced in hydrogen anneal to render microcapillary walls semiconducting and capable of sustaining charge replenishment from an external power supply. Previously, we reported electro-osmotic pumping characteristics of MCP where we also noticed a peculiar flow behavior that can be attributed to its semiconducting surface and faradaic reactions possibly engaged [25]. Inspired by this finding, the current study is set to investigate MCP for the characteristics of BPE focusing anionic tracer molecules in a microchannel.

1.2 Theory

Figure 1 depicts a typical segment of MCP and describes its working principle as a BPE membrane for the enrichment of anionic species within a microdevice built to harvest faradaic reactions. As seen from scanning electron microscope images in Fig. 1A, MCP packs in a glass matrix a highly dense and highly regular array of microcapillaries with fairly smooth sidewalls. Given their semiconducting sidewalls and high-aspect ratio structures, such cylindrical microcapillaries, each capable of serving as a tiny BPE, act in unison and thus expectedly lead to a rapid onset of a highly localized sharp field gradient and the subsequent effective enrichment of anionic species. In the device, MCP partitions a microchannel filled with an electrolyte buffer containing anionic species

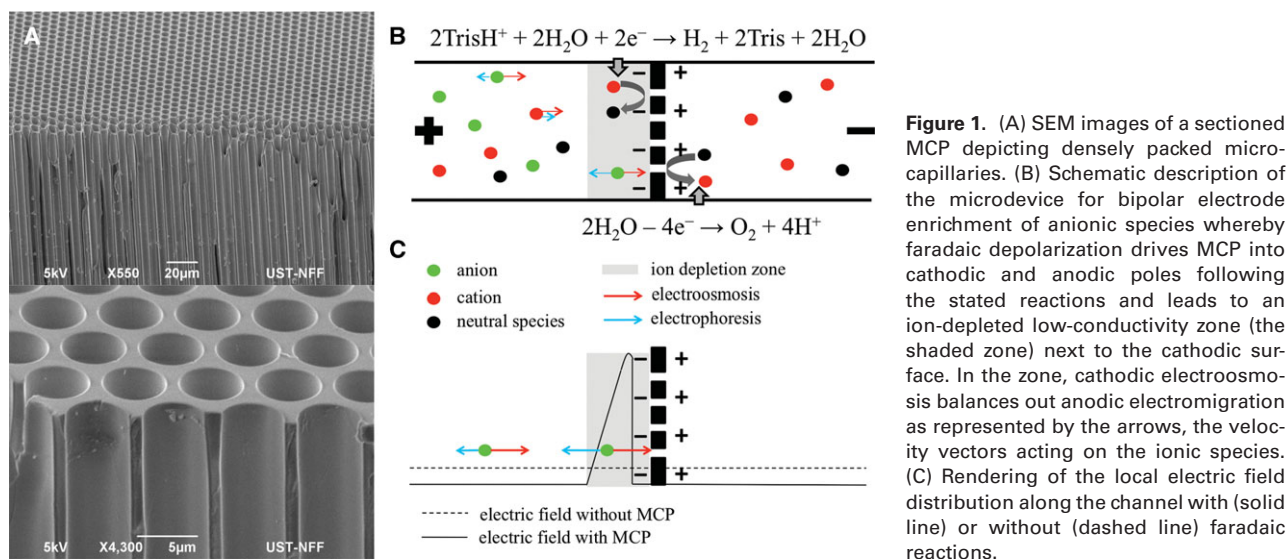
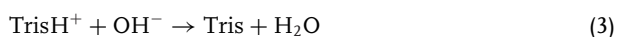
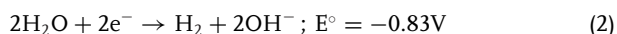
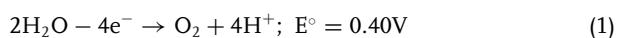


Figure 1. (A) SEM images of a sectioned MCP depicting densely packed microcapillaries. (B) Schematic description of the microdevice for bipolar electrode enrichment of anionic species whereby faradaic depolarization drives MCP into cathodic and anodic poles following the stated reactions and leads to an ion-depleted low-conductivity zone (the shaded zone) next to the cathodic surface. In the zone, cathodic electroosmosis balances out anodic electromigration as represented by the arrows, the velocity vectors acting on the ionic species. (C) Rendering of the local electric field distribution along the channel with (solid line) or without (dashed line) faradaic reactions.

to be enriched and across which a constant voltage bias is maintained. A potential drop of sufficient magnitude (with respect to the standard reduction potential E°) across MCP drives the coupled faradaic reactions in (1) and (2) at the anodic and cathodic poles, respectively [19, 21].



As stated in (3), hydroxide anions (OH^-) generated at the cathodic pole of MCP are neutralized by the buffer cations (TrisH^+). In consequence, a region of low conductivity develops in the vicinity of the cathodic pole and continuously extends into the anodic channel as indicated by the shaded zone in Fig. 1B and C. This is accompanied by an increase in the local electric field, rising up from a uniform profile therein (solid line versus dashed line in Fig 1C). The higher the conductivity contrasts across the depletion boundary, the sharper the field gradient, which can be managed by employing a high ionic-strength buffer and driving faradaic reactions faster. Species are transported in the channel from anode to cathode under the net influence of electroosmosis, which dominates their electromigration except in the depletion zone wherein anionic species are slowed down and enriched by the opposing electrophoretic forces amplified by the field.

2 Materials and methods

2.1 The device

Figure 2 presents an exploded view of the device schematics along with an assembled unit incorporating a fragment

of MCP depicted next to a whole intact sample (diameter 18 mm). All samples were purchased from Chairman Photoelectricity S&T Co., P. R. China, and contained nearly 12×10^6 microcapillaries each $6 \mu\text{m}$ in diameter across a glass plate $300 \mu\text{m}$ thick. As can be seen, the device with a single inlet and a single outlet was assembled by sandwiching a fragmented piece of MCP containing roughly 8.1×10^4 microcapillaries across an effective area of $\sim 3 \text{mm}^2$ between two identical hybrid microchannels, each 15 mm long, $50 \mu\text{m}$ wide, and $45 \mu\text{m}$ deep replica molded in PDMS (Sylgard 184, Dow Corning) following the standard soft-lithography procedure and then enclosed with a glass slide bonded over as a cover [26]. All the bonding steps were realized through activating the respective surfaces in oxygen plasma (29.6W Harrick Plasma) for 45 s. Prior to bonding, either PDMS slab was bored with a pair of holes 2 mm in diameter and 15 mm apart so as to allow fluidic access to the microchannels and MCP piece.

2.2 Reagents

Fluorescein (Fl^{2-} , Sigma-Aldrich, Hong Kong) was used in the experiments as a fluorescent tracer to measure the extent of enrichment process. Tris-HCl buffer was used as background electrolyte and prepared by diluting Trizma Base (Sigma-Aldrich) in DI water ($18.0 \text{M}\Omega \text{cm}$) to a desired concentration and with a pH level adjusted to 8.2 by HCl.

2.3 Instruments

Enrichment of Fl^{2-} was monitored through an epifluorescence microscope (FN1; Nikon, Japan) equipped with a mercury lamp (100 W), a filter cube set allowing for excitation at 492 nm and for emission above 520 nm, and a

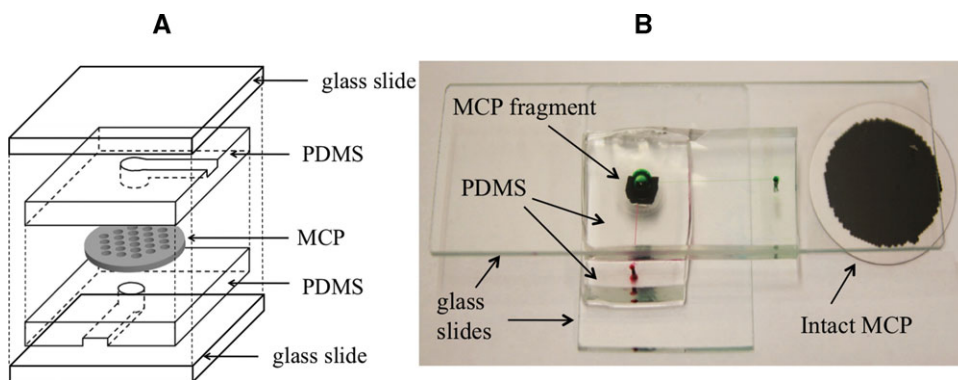


Figure 2. (A) Exploded view of the device schematics built for bipolar electrode focusing of anionic analytes and featuring a fragment of MCP sandwiched between a pair of identical hybrid microchannels in PDMS/glass. (B) Picture of an assembled device shown next to an intact MCP, the opaque disk with a porous region surrounded by a solid transparent glass border.

CCD camera (RT3 Mono; SPOT). Images of the enrichment were captured through a 10× objective lens and stored in a computer. Faradaic reactions were activated via platinum electrodes (Leego Precision Alloy, China) immersed into the reservoirs and connected to a high-voltage power supply (Tianjin Dongwen Co., China) controlled through LabView (National Instruments) software.

2.4 Experiments

Prior to each experiment, the device under test was rinsed with Tris-HCl buffer via vacuum pump connected to the either reservoir. Experiments were conducted upon replacing the rinsing buffer with Tris-HCl containing 100 pM, 1 nM, or 10 nM Fl^{2-} . During experiments, time-resolved video frames were acquired and analyzed for fluorescence intensity by an image processing software ImageJ (National Institutes of Health, Bethesda, MD, USA). Concentration of the enriched Fl^{2-} molecules was determined by comparing the band maximum intensity to a set of calibrated Fl^{2-} intensities. Dividing the concentration of the enriched band to the initial tracer concentration provided us with the enrichment factor (EF).

3 Results and discussion

3.1 Electroosmotic mobility

First, we investigate the influence of MCP on the EOF characteristics of the device using the neutral marker Rhodamine B (RhB) [27]. For the device assembled without MCP partitioning the channels, the electroosmotic mobility μ_{eof} measured using DI water is $0.95 \times 10^{-4} \text{ cm}^2 \text{ V}^{-1} \text{ s}^{-1}$ and compares well with the values reported earlier. For instance, a value of $1 \times 10^{-4} \text{ cm}^2 \text{ V}^{-1} \text{ s}^{-1}$ has been cited for native PDMS channels while slightly larger (by a factor of 1.4–1.8) for those hybrids, defined in part by PDMS and glass [28]. Also, a slight decline in the electroosmotic mobility is observed with the increased conductivity of Tris-HCl buffer upon replacing DI water (Fig. 3). Such trend is expected since the increased ionic strength of the buffer is known to modulate electrical double layer as well as the surface zeta potential, ζ [29, 30].

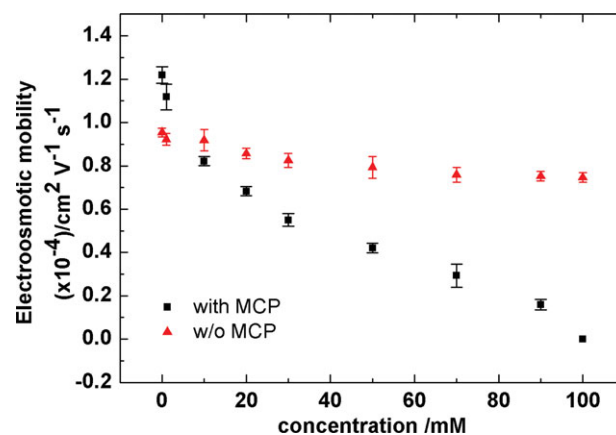


Figure 3. Plot of the electroosmotic mobility with or without microchannel plate partitioning the channels in the device as a function of Tris-HCl buffer concentration measured via neutral dye Rhodamine B. The lowest concentration is obtained by replacing Tris-HCl buffer with DI water.

Interestingly, though, the presence of MCP partitioning the channels in the device greatly alters EOF characteristics in a unique way. First and foremost, the electroosmotic mobility measured using DI water remains toward the cathode and yet limited to a value of only $1.22 \times 10^{-4} \text{ cm}^2 \text{ V}^{-1} \text{ s}^{-1}$, a fraction (~ 0.25) of those obtained with typical silica-based surfaces [31]. This suggests a value of ζ , -17.4 mV , as can be deduced from the expression, $\mu_{\text{eof}} = \epsilon\zeta/\eta$, where ϵ is the permittivity of water $\sim 7 \times 10^{-10} \text{ F/m}$ and η is the viscosity of water $1 \times 10^{-3} \text{ Pa s}$. This is fairly close to -15 mV , the value we previously reported based on the measurement of maximum EOF rate per unit effective voltage dropped across MCP [25].

Second, the decline in the electroosmotic mobility with the increased ionic strength of the buffer is far more dramatic when MCP is in the device partitioning the channels rather than left outside. The bulk flow practically comes to a stand still as the concentration of the buffer reaches 100 mM. This unique characteristic can be attributed to the semiconducting nature of microcapillary walls in MCP along with their ability to sustain bipolar faradaic processes at their opposing extremities. Duval and colleagues earlier proposed the manipulation of electroosmotic velocity field within an electron-conducting cylindrical microcapillary by engaging bipolar faradaic

reactions and suggested a theoretical framework for the analysis of the subsequent EOF, wherein the electrical double layer and ζ potential are defined by two concomitant mechanisms: a chemical charging process, which has its origins in protonation and deprotonation of surface amphoteric groups and an electrochemical charging process, which arises from polarization of the electron-conducting surface and bipolar faradaic reactions associated with it [32, 33]. Due to the intricate and nonlinear coupling of these two mechanisms, spatial inhomogeneities of electric field and of ζ potential begin to develop and ultimately lead to a hydraulic pressure gradient that can cause the reversal of the flow within localized domains throughout such microcapillaries. As the ionic strength of the buffer increases, the bipolar current becomes more dominant than the ohmic current, thereby leading to a more profound heterogeneous distribution of electric field and of ζ potential which, we believe, is responsible for the pressure-induced counter streams strong enough to oppose the bulk EOF. It should be noted that the subsequent experiments use 1 mM buffer with the electroosmotic mobility comparable to that of DI water and also with the current density limited such that no visible bubbles are formed up to 1000 V.

3.2 Concentration enrichment

Figure 4A shows a representative band of Fl^{2-} upon a 13 400-fold enrichment obtained by a voltage bias of 800 V maintained for 70 s across the device filled with an initial concentration of 1 nM Fl^{2-} in a buffer of 1 mM Tris-HCl (pH 8.2). The band is formed between the cathodic pole of MCP and the anode at a unique position where the bulk EOF toward the cathode is counter-offset by the electrophoretic motion of the dye molecules toward the anode. Figure 4B

reveals the dynamics of the enrichment process as the profile of the enriched zone evolves over time with the corresponding peak becoming more and more intense and approaching closer to MCP while relatively preserving its baseline width. This somewhat deviates from the trend observed in a microchannel embedded with a planar BPE wherein the corresponding peak becomes also broader [18, 22] as it gets more intense and may appear moving in the opposite direction [18]. Such opposite movement of the peak away from BPE suggests that the spatially extended ion-depletion region could be still building up. Here, this region, however, quickly stabilizes within 50 s from the voltage bias onset (see the movie clip in Supporting Information). Beyond 50 s, the peak intensity continually increases as long as the voltage bias is maintained until 150 s from the voltage onset when it begins to stabilize again at a position closer to MCP. This slight shift in the peak position toward MCP along with the saturation in the peak intensity is attributed to the reduced electrophoretic velocity field as the enriched anions increase the ionic strength of the depleted region, thereby degrading the field gradient accordingly [6, 22]. We believe that the enrichment performance reported here that is the exceptionally rapid initiation and stabilization of a fairly sharp peak of the enriched molecules, unlike of those obtained with a planar BPE, is a result of the high-porosity 3D structure offered by the semiconducting MCP.

Subsequent experiments investigate the change in the peak intensity for three distinct initial concentrations either as a function of time at a fixed bias voltage or as a function of bias voltage applied for a fixed time period. Figure 4C shares a set of curves describing the time evolution of the peak intensity during 800 V bias presenting the values of EF with respect to the initial concentrations of Fl^{2-} . With an initial concentration of 10 nM and 1 nM Fl^{2-} , EF reaches a plateau

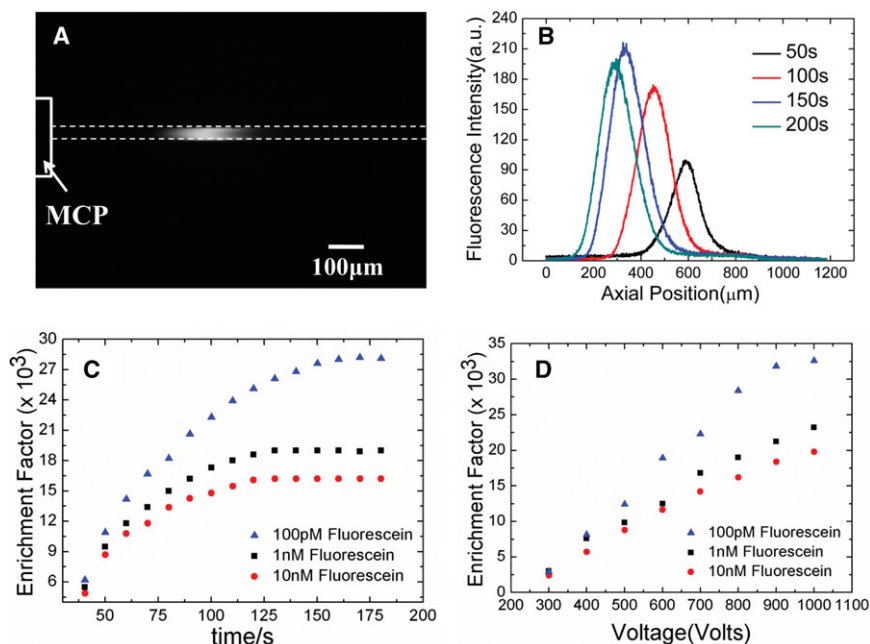


Figure 4. (A) Fluorescent micrograph of a typical band upon 13400-fold enrichment from an initial concentration of 1 nM fluorescein (Fl^{2-}) in a buffer of 1 mM Tris-HCl (pH 8.2) via 800 V maintained for 70 s. (B) For the same experiment, time evolution of the fluorescence intensity distribution along the anodic microchannel at axial positions measured from the cathodic side of microchannel plate and captured at the specified time intervals (the legend) since the onset of the applied voltage bias (800 V). (C, D) Enrichment factors calculated based on the measured peak intensities and presented either (C) as a function of time at 800 V bias or (D) as a function of bias voltage at the conclusion of 200 s from the onset across the device for three distinct initial concentrations of Fl^{2-} (the legend) in 1 mM Tris-HCl buffer (pH 8.2).

in 130 s registering 16 000- and 19 000-fold enrichment at an average rate of 123- and 146-fold/s, respectively. Lowering the initial concentration to 100 pM allows the enriched zone more time to saturate, which occurs at a concentration comparable to that of background ions and disruptive to the established field gradient. Thus, EF further rises 28 000-fold in 160 s, at 175-fold/s. In comparison, Ross and Locascio employing temperature gradient focusing achieved 11 250-fold at a rate of 1.9-fold/s [11]. Humble et al. [15] and then Liu et al. [16], both using electric FGF, demonstrated 10 000-fold at 4.17-fold/s and 4000-fold at 1.1-fold/s, respectively. Anand et al., using a planar BPE in a dual-channel arrangement, the so-called “faradaic ICP”, attained 55 000-fold at 27-fold/s and 142 000-fold at 71-fold/s for the initial tracer concentration of 1 nM and 10 pM, respectively [23]. The latter is the highest rate of enrichment reported by the authors based on BPE and exceeds the rate, 28-fold/s, obtained with a traditional ICP at micro/nanochannel junctions using a comparable initial analyte concentration 33 pM [6]. Interestingly, though, the rate reported here, 175-fold/s, is remarkable in view of the fact that it is achievable under less favorable conditions as opposed to those surrounding the faradaic ICP that attained a rate of 71-fold/s: our average field strength 267 V/cm versus 417 V/cm, Tris buffer 1 mM versus 100 mM, and the initial tracer concentration 100 pM versus 10 pM.

Saturation in enrichment for a fixed bias voltage is an expected outcome since the presence of the enriched anionic molecules in the ion-depleted region poses a destabilizing effect on the established ionic strength and the accompanying field gradient [6, 22]. This, however, can be overcome by increasing the bias voltage. Figure 4D reveals the relation between the bias voltage and maximum EF obtained at saturation, 200 s from the bias onset. Maximum EF rises with the bias voltage more or less linearly and mostly remains independent of the initial tracer concentration for the values below 500 V. Above 500 V, however, it rises considerably fast for the lowest initial concentration (100 pM). With an increased bias, electroosmotic bulk flow in the anodic segment becomes far more dominant over electrophoretic motion of the tracer, assuring a faster transport of the tracer to the focusing zone. Meanwhile, in the focusing zone, both opposite forces equilibrate at an increased strength, mounting their sequestering effects on the enriched band. Local electrophoretic strength increases because, with a larger bias, faradaic currents intensify and, through faster OH⁻ production and subsequent TrisH⁺ neutralization, lead to a sharper transition in the ionic strength of the depletion zone boundary, thereby establishing a steeper field gradient. Further rise in EF is expected with even larger bias but usually hindered by the generation and accumulation of bubbles on the surface of MCP (more than 1000 V).

4 Concluding remarks

We have demonstrated that the MCP, traditionally employed as an electron multiplier in image intensifiers, can be adopted

without any modification as a highly effective BPE driving faradaic reactions in an electrolyte buffer, owing to its high-porosity 3D structure with a semiconducting surface. One could harvest such faradaic reactions using microfluidics and focus anionic species at a fairly rapid rate by establishing an ion-depletion zone with a sharp field gradient balancing electromigration against electroosmosis. Constructed typically in lead glass with a compact and planar format, MCP can be treated as a glass slide and bonded with PDMS-based microfluidics upon oxygen-plasma surface activation. Readily available from various suppliers covering a range of specifications (e.g., pore size), MCP takes away the burden and requirement of having an access to sophisticated cleanroom facilities for the fabrication of such an intricate structure that would otherwise have to face complications from metallization, lithography-based patterning, and deep reactive ion etching (DRIE). As a material and structure, MCP is quite robust and highly regular in pore distribution, hence exhibiting a compact and stable depletion zone and the consequent sharp enrichment peaks. The high-performance characteristics of MCP shown could be beneficial for the rapid enrichment and detection of charged biomarkers including DNA and proteins in bioanalytical microdevices.

This project was financially supported by the Startup Grant from the Electronic and Computer Engineering Department, Hong Kong University of Science and Technology.

The authors have declared no conflict of interest.

5 References

- [1] Whitesides, G. M., *Nature* 2006, 442, 368–373.
- [2] Liang, Z., Chiem, N., Ocvirk, G., Tang, T., Fluri, K., Harrison, D. J., *Anal. Chem.* 1996, 68, 1040–1046.
- [3] Tokeshi, M., Minagawa, T., Kitamori, T., *Anal. Chem.* 2000, 72, 1711–1714.
- [4] Ramsey, J. D., Collins, G. E., *Anal. Chem.* 2005, 77, 6664–6670.
- [5] Long, Z. C., Liu, D. Y., Ye, N. N., Qin, J. H., Lin, B. C., *Electrophoresis*, 2006, 27, 4927–4934.
- [6] Wang, Y. C., Stevens, A. L., Han, J. Y., *Anal. Chem.*, 2005, 77, 4293–4299.
- [7] Hofmann, O., Che, D. P., Cruickshank, K. A., Muller, U. R., *Anal. Chem.* 1999, 71, 678–686.
- [8] Chien, R. L., Burgi, D. S., *J. Chromatogr.* 1991, 559, 141–152.
- [9] Jacobson, S. C., Ramsey, J. M., *Electrophoresis* 1995, 16, 481–486.
- [10] Walker, P. A., Morris, M. D., Burns, M. A., Johnson, B. N., *Anal. Chem.* 1998, 70, 3766–3769.
- [11] Ross, D., Locascio, L. E., *Anal. Chem.* 2002, 74, 2556–2564.
- [12] Balss, K. M., Vreeland, W. N., Phinney, K. W., Ross, D., *Anal. Chem.* 2004, 76, 7243–7249.

- [13] Greenlee, R. D., Ivory, C. F., *Biotechnol. Prog.* 1998, 14, 300–309.
- [14] Koegler, W. S., Ivory, C. F., *J. Chromatogr. A* 1996, 726, 229–236.
- [15] Humble, P. H., Kelly, R. T., Woolley, A. T., Tolley, H. D., Lee, M. L., *Anal. Chem.* 2004, 76, 5641–5648.
- [16] Liu, J., Sun, X., Farnsworth, P. B., Lee, M. L., *Anal. Chem.* 2006, 78, 4654–4662.
- [17] Huang, Z., Ivory, C. F., *Anal. Chem.* 1999, 71, 1628–1632.
- [18] Dhopeswarkar, R., Hlushkou, D., Nguyen, M., Tallarek, U., Crooks, R. M., *J. Am. Chem. Soc.* 2008, 130, 10480–10481.
- [19] Hlushkou, D., Perdue, R. K., Dhopeswarkar, R., Crooks, R. M., Tallarek, U., *Lab Chip* 2009, 13, 1903–1913.
- [20] Laws, D. R., Hlushkou, D., Perdue, R. K., Tallarek, U., Crooks, R. M., *Anal. Chem.* 2009, 81, 8923–8929.
- [21] Perdue, R. K., Laws, D. R., Hlushkou, D., Tallarek, U., Crooks, R. M., *Anal. Chem.* 2009, 81, 10149–10155.
- [22] Anand, R. K., Sheridan, E., Hlushkou, D., Tallarek, U., Crooks, R. M., *Lab Chip* 2011, 11, 518–527.
- [23] Anand, R. K., Sheridan, E., Knust, K. N., Crooks, R. M., *Anal. Chem.* 2011, 83, 2351–2358.
- [24] Wiza, J. L., *Nucl. Instrum. Methods* 1979, 162, 587–601.
- [25] Cao, Z., Yuan, L., Liu, Y. F., Yao, S., Yobas, L., *Microfluid. Nanofluid.*, 2012, 13, 279–288.
- [26] McDonald, J. C., Whitesides, G. M., *Accounts Chem. Res.* 2002, 35, 491–499.
- [27] Lukacs, K. D., Jorgenson, J. W., *HRC-J. High Res. Chrom.* 1985, 8, 407–411.
- [28] Ren, X. Q., Bachman, M., Sims, C., Li, G. P., Allbritton, N., *J. Chromatogr. B* 2001, 762, 117–125.
- [29] VanOrman, B. B., Liversidge, G. G., McIntire, G. L., Olefirowicz, T. M., Ewing, A. G., *J. Microcol. Separat.* 1990, 2, 176–180.
- [30] Gaudioso, J., Craighead, H. G., *J. Chromatogr. A* 2002, 971, 249–253.
- [31] Harrison, D. J., Manz, A., Fan, Z., Luid, H., Widmers, H. M., *Anal. Chem.*, 1992, 64, 1926–1932.
- [32] Duval, J. F. L., *J. Coll. Interf. Sci.* 2004, 269, 211–223.
- [33] Qian, S., Duval, J. F. L., *J. Coll. Interf. Sci.* 2006, 297, 341–352.